Contact Stability Analysis of Virtual Walls

Lonnie Love and Wayne Book

The George Woodruff School of Mechanical Engineering
Georgia Institute of Technology
Atlanta, GA 30332-0405

Abstract

Haptic interfaces are mechanical systems coupled to humans. These devices provide a method of relaying mechanical information between a human and a computer generated environment. A basic element in any virtual environment is the virtual wall. The problem addressed in this research is the stability of haptic interfaces when simulating virtual walls. Many researchers have recently published reports describing an unmodeled vibration experienced when attempting to simulate stiff surfaces. This investigation focuses on the structure of the control algorithm and its discrete time implementation. A computed torque method of impedance control provides robust performance, but is limited due to discrete time implementation. Bounds on the target impedance are defined though Jury analysis.

1. Introduction

Haptic interfaces are robotic systems coupled to humans to provide physical stimulation. Classic applications of such devices include bilateral teleoperation and active joystick control in performance aircraft. A few new and exotic applications include physical conditioning and surgical simulation. A primary element of any environment is the wall. In a virtual environment, walls constrain the motion of an operator. Researchers have recently acknowledged the possibility of vibration during simulation of stiff environments. Kazerooni (1993) analyzes the stability of humans coupled to haptic interfaces. He describes a periodic motion that exists for general virtual environments. He attributes this effect to time delays between the input force and the response of the haptic interface. The general solution he proposes is to increase the sample rate of the controller to a sufficiently high value, beyond 350Hz for his system. Colgate and Schenkel (1994) use passivity to analyze the stability of a single degree of freedom haptic interface with a discrete time controller. Colgate and Brown (1994) extend this work to define the "Z-Width" of a haptic interface. This establishes the dynamic range of impedances achievable by the haptic interface. Their analysis suggests a lower bound on the inherent damping of the device. Our work takes a slightly different approach to the stability analysis. We use Jury stability criteria to define the relationship between the target stiffness, damping and sampling rate of a computed torque impedance controlled haptic interface. Our analysis corresponds with the results described by Kazerooni and Colgate. There is an upper threshold on the stiffness of the virtual wall that is a function of the sampling rate of the controller. However, we also find that there is an upper, as well as a lower bound on the target damping of the system. A series of experiments illustrate the predicted trends in the stability of a haptic interface as a function of the target stiffness, damping and sampling rate.

2. Control implementation

One primary objective of a haptic interface is to control the resistance between the operator and the device. Impedance control provides a seamless method of obtaining this goal (Hogan 1985). The formulation of the control scheme is based upon defining a target impedance for the robot.

A survey of the literature suggests that there are two popular methods of implementing impedance control: Target Model Reference Control (TMRC) and Computed Torque control. The TMRC structure couples standard robot motion control techniques to an outer impedance control loop. The command trajectory to the servo controller combines the initial desired trajectory with a force disturbance response based upon the desired impedance. The second method uses a computed torque robot controller. This technique uses feedback linearization to compensate for the robot's natural dynamics and provide additional compensation to control the effective impedance of the manipulator. Our work focuses on the stability, using Jury stability criteria, of computed torque impedance control used for haptic interfaces.

2.1 Computed Torque Impedance Control

Computed torque impedance control uses feedback linearization to provide compensation for a robot's natural dynamics. This may include gravitational and inertial effects, and nonlinear components such as the coriolis and centripetal forces. Additional compensation is provided to produce an effective impedance at the end effector of a manipulator.

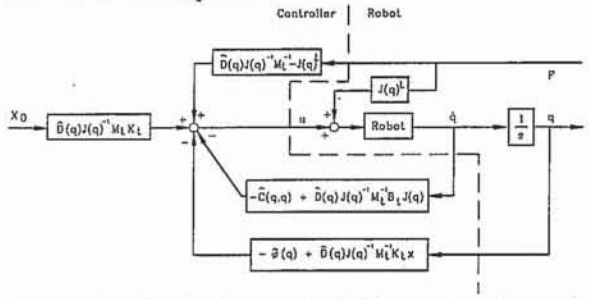

Figure 1: Block Diagram for CT Impedance Control

The performance obtained using this method hinges upon the parametric and nonparametric accuracy of the model of the robotic system.

3. Case Study: Stiff Wall

A case study based upon discontinuous environments is performed. Figure 2 illustrates the system studied. The mass with damping represents a single degree of freedom manipulator. The force u provides the control, while F represents an external force applied to the robot. For the haptic interface, this external force is generated by the human. Figure 3 illustrates the environment that the haptic interface is to simulate. The spring-mass-dashpot represents the target impedance of the manipulator.

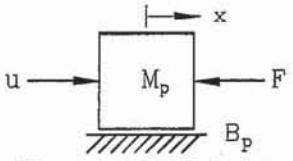

Figure 2: 1 DOF Robot

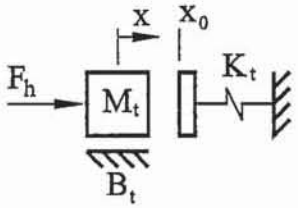

Figure 3: Target Impedance

When the operator moves the display beyond the constraint surface of the virtual wall at x_0, the target stiffness of the robot is K_t. Equation (1) describes a simple model representing the wall.

$$K_t(x) = \frac{K_t}{2}(1 + \text{sign}(x - x_0)) \qquad (1)$$

The parameters used in this study are based upon the characteristics of a two degree of freedom robot located in the Intelligent Machines and Dynamics Laboratory at Georgia Tech (Love 1994). For this study, only one degree of freedom is considered. The effective mass and damping at the tip of the robot are 14.3kg and 78.4 N/m/s respectively. Furthermore, the human is modeled only as an external source of force on the haptic interface.

4. Stability of Computed Torque Controller

Based upon the design specifications, the computed torque paradigm provides the following control law.

$$u = (M_p M_t^{-1} - 1) F_h - (M_p M_t^{-1} B_t - B_p)\dot{x} - \frac{1}{2} M_p M_t^{-1} K_t (1 + \text{sign}(x - x_0))(x - x_0) \qquad (2)$$

Fasse and Hogan (1989) used Lyaponov stability criteria to illustrate that an impedance controlled robot will be stable when interacting with a passive environment. Thus, an analog implementation of the computed torque method is stable for all target wall stiffness. Parametric uncertainty degrades performance, but has little effect on stability. However, nonparametric uncertainty, such as unmodeled joint compliance, can reduce the bandwidth of the system and potentially destabilize the system (Colgate 1989).

4.1 Discrete time implementation

Modern control techniques rely heavily on the use of computers for control computations. Many sophisticated control techniques in use today would not be possible without the use of computers. Quantization, discrete time sampling and control, and saturation are only a few of the limitations associated with real-time control (Hanselman 1987).

Consider the example described in section 3. An impedance controlled manipulator contacts a stiff surface. Lyaponov stability criterion states that if the target stiffness, damping, and mass are positive definite and the environment is passive, the coupled system will be asymptotically stable (Fasse and Hogan 1989). Figure 4 illustrates the phase-plane of such a system, using a continuous time control. As expected, the system is oscillatory, but asymptotically stable. The same controller is modeled using a discrete time controller. The resulting phase-plane, illustrated in Figure 5, suggests that a limit cycle exists when using a

discrete time implementation of this controller. The need for discrete time stability analysis is evident through this simple example. Figure 5 illustrates a hybrid block diagram of the computed torque impedance controlled robot.

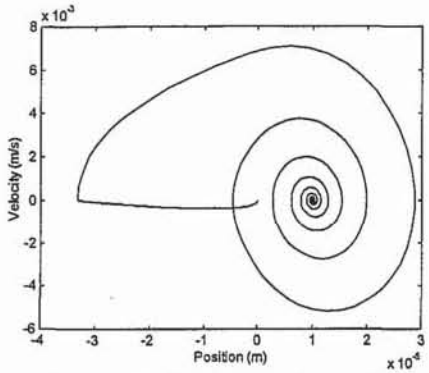

Figure 4: Continuous Controller Phase Plane

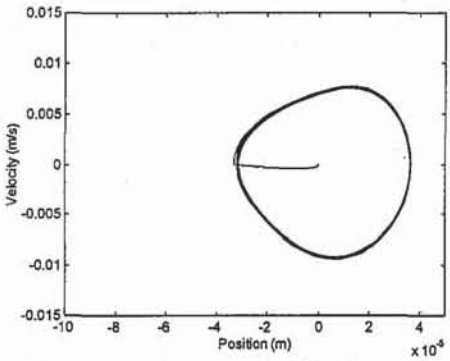

Figure 5: Discrete Controller Phase-Plane

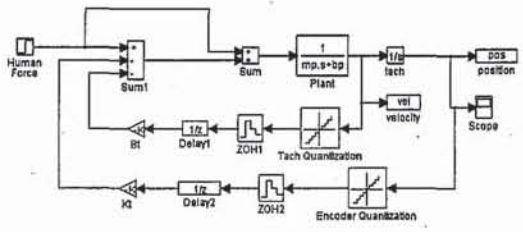

Figure 6: Discrete Time Block Diagram of CT Impedance Controller w/Wall

Our approach to the stability analysis of haptic interfaces uses Jury's test to define the limits on parameters that ensure BIBO stability. This analysis focuses on the effect variations in the target stiffness, damping and sampling rate have on stability. Jury's test is similar in structure to Routh's stability test for continuous time systems (Jury 1964). First, the block diagram in Figure 6 is reduced to provide the system's characteristic equation, Eq.(3). Next, known parameters such as the systems mass and damping are substituted into Eq.(3), providing an expression of the characteristic equation in terms of the haptic interface's target impedance.

$$1-\left(1+e^{B_p T/M_p}\right)z^{-1}+\left[\left(\frac{M_p}{M_t}\frac{B_t}{B_p}-1\right)\left(1-e^{B_p T/M_p}\right)+e^{-B_p T/M_p}\right]z^{-2}$$
$$+\left(1-e^{-B_p T/M_p}\right)\left[\frac{M_p}{M_t}\frac{K_t T}{B_p}-\frac{M_p}{M_t}\frac{B_t}{B_p}+1\right]z^{-3}=0 \qquad (3)$$

$$a_1=-\left(1+e^{-B_p T/M_p}\right)$$
$$a_2=\left(1-e^{-B_p T/M_p}\right)\left(\frac{M_p}{M_t}\frac{B_t}{B_p}-1\right)+e^{-B_p T/M_p} \qquad (4)$$
$$a_3=\left(1-e^{-B_p T/M_p}\right)\left[\frac{M_p}{M_t}\frac{K_t T}{B_p}-\frac{M_p}{M_t}\frac{B_t}{B_p}+1\right]$$

The characteristic equation in Eq. (3), after substitution of the variables in Eq. (4), reduces to the expression in Eq. (5).

$$1+a_1 z^{-1}+a_2 z^{-2}+a_3 z^{-3}=0 \qquad (5)$$

Jury's test consists of finding the bound on a parameter of the system that satisfies the conditions in Eq. (6)

$$b_0>0,\ c_0>0,\ d_0>0 \qquad (6)$$

where

$$b_0=1-a_3^2$$
$$b_1=a_1-a_2 a_3$$
$$b_2=a_2-a_1 a_3$$
$$c_0=b_0-\frac{b_2^2}{b_0} \qquad (7)$$
$$c_1=b_1-\frac{b_1 b_2}{b_0}$$
$$d_0=c_0-\frac{c_1^2}{c_0}$$

Since this investigation focuses on the target stiffness and damping of the haptic interface, the target mass of the haptic interface is fixed at 5 kg. The target damping and stiffness are varied over a desired range and Jury's test provides the maximum sampling rate that ensures BIBO stability. Figure 7 illustrates the maximum sampling rate as a function of the target stiffness and damping of the robot. This contour provides a graphical representation of the haptic interface's Z-width.

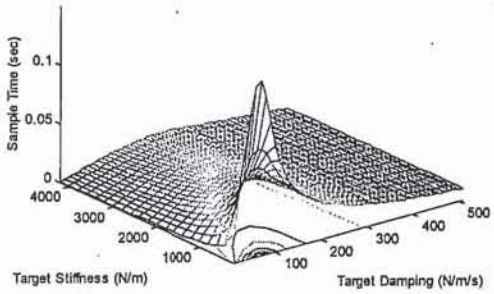

Figure 7: Limits of B_t and K_t with M_t= 5 kg

6. Experimental Results

The following series of experiments use Jury's test to establish the limit of the target stiffness and damping. The initial target mass and damping of the robot are 5 kg and 141 N/m/s respectively with an initial sampling frequency of 100 Hz. Substitution of these parameters into Eq.(4), provides the parameters of the characteristic equation in terms of the target stiffness of the virtual wall. Bounds on this stiffness are established through the constraints in Eq.(6). Figure 8 illustrates the stability constraint variables as a function of the target stiffness. A violation of the constraint occurs when either b0, c0, or d0 is less than zero. Inspection of these values suggests that the system should be stable until K_t exceeds 6710 N/m.

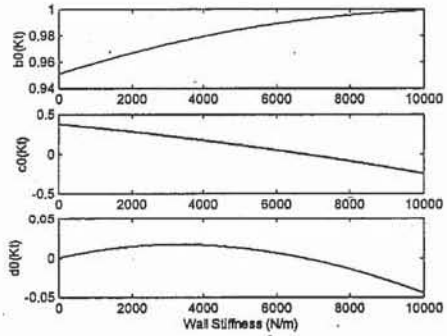

Figure 8: Stability Coefficients for F_s=100Hz

Figure 9 illustrates the measured position and velocity response of the experimental platform simulating a virtual wall. The vertical wall has a stiffness of 6700 N/m and is located 0.762 m from the base of the robot. The sampling rate of the controller is 100 Hz. Figure 10 illustrates the position and velocity response of the system when the wall stiffness is 11 kN/m. The dynamics of the human, which are not explicitly modeled here, may influence the stability of the system and partially explain the delayed onset of unstable behavior.

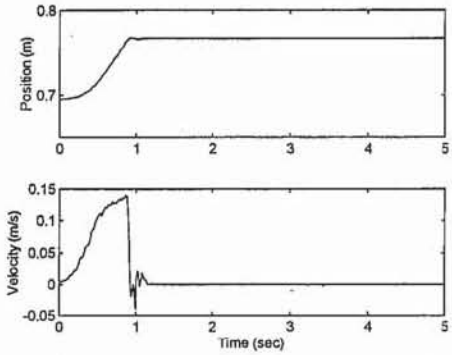

Figure 9: Kt = 6.7kN/m, Fs=100Hz

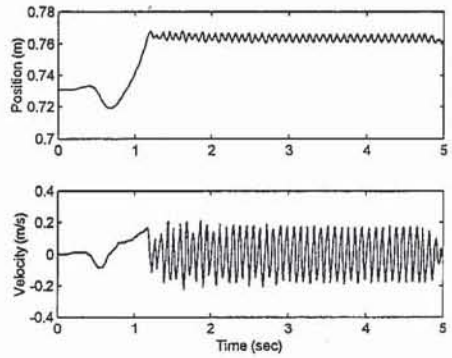

Figure 10: Kt = 11kN/m, Fs=100Hz

Stability is regained by increasing the sample rate, as predicted by the contour in Figure 7. Figure 11 illustrates the response of the system when the sample rate is increased to 1000 Hz and the wall stiffness is 32.7kN/m. Repeating the stability analysis described above with a sampling rate of 1kHz, the system should go unstable when the wall stiffness exceeds 70.2 kN/m. Experiments suggest that a slight vibration begins to influence the response when the stiffness exceeds 90kN/m, illustrated in Figure 12..

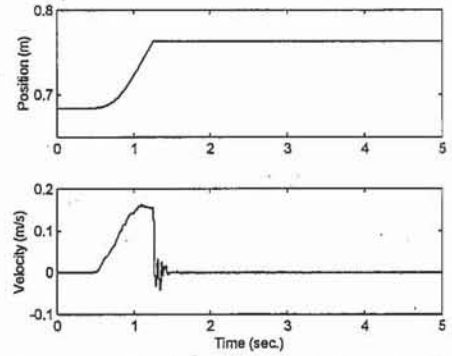

Figure 11: Wall Stiffness 36kN/m, Fs=1kHz

Hanselmann, H., 1987, "Implementation of Digital Controllers," *Automatica*, January, Vol. 23, pp.7-32.

Hogan, N., 1985, "Impedance Control: An Approach to Manipulation: Part II - Implementation," *Journal of Dynamic Systems, Measurement and Control,* March 1985, Vol. 107, No. 1, pp.8-16.

Jury, E.,I., 1964, "Theory and Application of the Z-Transform Method," J.Wiley, New York.

Kazerooni, H., 1993, "Human Induced Instability in Haptic Interfaces," *ASME-WAM*, DSC-Vol. 49, pp.15-27.

Love, L., and Book, W., 1994, "Design and Control of a Multiple Degree of Freedom Haptic Interface," *ASME-WAM*, DSC-Vol.55-2, pp.851-856.